Kidney International, Vol. 50 (1996), pp. 783–795

Early defect in branching morphogenesis of the ureteric bud in induced nephron deficit

THIERRY GILBERT, CHRISTIAN CIBERT, EVELYNE MOREAU, GÉRARD GÉRAUD, and CLAUDIE MERLET-BÉNICHOU

INSERM U.319, Développement Normal et Pathologique des Fonctions Épithéliales, and Département de Biologie du Développement, Laboratoire de Physiologie du Développement, Institut Jacques Monod, Université Paris 7-Denis Diderot, Paris, France

Early defect in branching morphogenesis of the ureteric bud in induced nephron deficit. Development of the metanephric kidney during embryogenesis can be altered both *in vivo* and *in vitro* by exposure to gentamicin, which may lead to oligonephronia. To study the role of the ureteric bud in nephron deficit genesis, we used metanephros organ cultures exposed to gentamicin as a model of impaired nephrogenesis. Ultrastructural localization of the antibiotic showed that by eight hours it was already present within the epithelial cells of the ureteric bud and in its growing ends, and also trapped in the adjacent blastema. Using confocal microscopy and image analysis, we devised a quantitative approach to analyze the branching pattern of the ureteric bud, and showed that by 24 hours of culture, despite no change of explants growth, gentamicin had significantly decreased the number of branching points. This effect involved the early branching events and was limited to end buds that had no nephron anlagen nearby. Our findings indicate that impaired branching morphogenesis of the ureteric bud is the likely event of gentamicin-induced nephron deficit.

In mammalian embryogenesis, the inductive interaction between the ureteric bud and the metanephric blastema is the initial event that will result in metanephros formation whose further development and differentiation will form the adult kidney [reviewed in 1, 2]. The ureteric bud morphogenesis and outgrowth in the undifferentiated metanephric blastema require close epithelium-mesenchyme interactions and play central roles in conditioning the genesis of nephrons [3]. The configuration of branching tubules with swollen end-buds in contact with a mesenchyme ensues the normal development of many organs, such as the mammary glands, salivary glands, pancreas and lungs [4–7]. In the kidney, the metanephrogenic mesenchyme not only plays a role in conditioning branching morphogenesis of the collecting duct tree, but it has also the distinctive feature to receive signals from the ureteric bud to be further converted into multiple filtering units, the nephrons [2, 8]. The nature of the signals involved in these reciprocal inductions between the ureteric bud and the mesenchyme is still not fully identified. While the mechanisms of mesenchymal-epithelial conversion have been extensively studied [reviewed in 9, 10], little attention has been focused on the differentiation of the ureteric bud. However, it is clear that any disturbance of the ureteric bud outgrowth during renal organogenesis and/or its branching pattern may lead to renal malformation and various degree of oligonephronia.

Inborn nephron deficits have been reported. According to their severity, they may either initiate a progressive renal disease or influence the rate of progression of acquired renal disease [11]. The etiology of inborn nephron deficits is unknown, although recent studies in humans and animals have shown that intrauterine growth retardation might be a major cause of inborn nephron deficit [12, 13]. In humans, abnormal nephrogenesis has also been associated with *in utero* exposure to several drugs such as aminoglycosides and corticosteroids [14]. In rats, fetal exposure to gentamicin has been reported to induce ultrastructural damages in the nephrogenic zone and to cause permanent nephron deficit [15, 16]. Recently, we have been successful in reproducing this defect of nephrogenesis *in vitro* using rat metanephros organ culture, which makes this model suitable for investigating the cellular mechanisms leading to oligonephronia [17]. In both approaches, aminoglycoside accumulation found in the developing kidney turned out to be lower than that measured in the kidneys of human fetuses after a single dose of aminoglycosides to their mothers [16–19].

In this study, we used gentamicin-exposed metanephros organ culture as a tool for investigating the role of the ureteric bud in the genesis of oligonephronia. Growth and cell proliferation parameters were first determined, and we used immunoelectron microscopy to study the cellular targets of the antibiotic. Branching morphogenesis of the ureteric bud was then examined using specific labeling and confocal microscopy. Using image analysis, the skeleton of the ureteric bud was generated in order to characterize its branching pattern. This methodology turned out to be extremely sensitive and allowed us to show that, at the early stages of metanephros development, the ureteric bud ability to branch, but not to elongate, was altered within the first hours of culture in gentamicin-exposed metanephros. In turn this may explain the reduced nephrogenesis. Additionally we provide evidence for a differential sensitivity to gentamicin of the ureteric bud ends according to their location.

Received for publication November 13, 1995
and in revised form February 16, 1996
Accepted for publication March 21, 1996

Methods

Metanephros organ culture

We used the previously described rat metanephros organ culture system [17, 20]. Briefly, dated pregnant Sprague-Dawley

female rats (Charles River, Paris, France) were anesthetized on day 14 of gestation (day zero is the day following mating) with sodium pentobarbital and embryos (E14) were collected. Intact metanephroi were aseptically removed and placed onto a 0.8 μm Millipore AA filter (Millipore, Saint-Quentin-en-Yvelynes, France), floating on a serum-free medium. The latter consisted of DMEM/Ham's F12 (vol/vol) containing 15 mM HEPES and 45 mM sodium bicarbonate (pH 7.45 ± 0.05). According to Avner et al [21], this medium was supplemented with transferrin 6.2×10^{-8} M, selenium 6.8×10^{-9} M, insulin 8.3×10^{-7} M, triiodothyronine 2×10^{-9} M and prostaglandin E_1 7×10^{-8} M to ensue optimal differentiation. The explanted metanephroi were cultured for two days at 37°C in a humidified incubator with 5% CO_2. Culture medium was changed daily. All reagents were purchased from Sigma. No antibiotic or fungicide was present in the control culture medium.

In order to counteract the interassay variability due to *in vitro* behavior heterogeneity of metanephroi explanted from different fetuses, we first selected E14 fetuses from whole litter mean weight of 140 ± 10 mg, and secondly, paired experiments were performed. For each fetus, one metanephros was grown as a control in medium without gentamicin, and the other grown in medium supplemented with 50 μg/ml gentamicin. This dose was chosen according to its efficiency to induce a nephron reduction greater than 20% in three out of four E14 metanephros organ cultures as compared to paired controls [17].

Assessment of metanephric growth

Growth of the explanted metanephroi was evaluated through determination of changes in their protein and DNA contents, and their surface area. The latter was expressed either in square millimeter when measured using a video camera coupled to a microcomputer, or in pixels in the instance of optical sections generated by the confocal microscope. Then, the explants were unmounted, rinsed three times in distilled water, sonicated in 150 mM saline for 30 seconds and assayed for protein determination according to Lowry's procedure with globin as standard. DNA was measured using Labarca and Peigen assay [22]. Data are expressed as μg protein or DNA per explant.

Cell proliferation was estimated by ^{3}H-thymidine incorporation at various times of culture. One-hour incubation steps were performed with 10 μCi of ^{3}H-thymidine (specific activity: 1 mCi/mmol) at 0, 7, 23 and 47 hours of culture. At each time point, nonspecific incorporation was monitored on metanephric explants incubated at 4°C with chilled ^{3}H-thymidine for one hour. After an overnight wash at 4°C, kidney rudiments were sonicated, and radioactivity assessed by liquid scintillation. Data are expressed as cpm per explant.

Determination of the mitotic index was carried out on two histological plastic sections 20 μm apart in the central region of each metanephric explant, and four distinct areas were examined: the mature epithelial ureteric duct, the growing extremities of the bud, the induced mesenchyme at the periphery of the end buds, and the non-induced metanephric blastema underneath the renal capsula. In each area, about one thousand cells were observed for each sample.

Light and electron microscopy

After 8, 24 and 48 hours of culture, metanephric explants were fixed by immersion with 2.5% glutaraldehyde (wt/vol) in 0.1 M cacodylate buffer, pH 7.4. After overnight washing in the same buffer at 4°C, they were postfixed in 1% osmium tetroxide (wt/vol), dehydrated through a series of graded ethanol, infiltrated and flat embedded in Epon. For histologic examination, 1-μm thick sections were cut parallel to the filter and stained with toluidine blue. For ultrastructural examination, ultrathin sections (~75 nm) were stained with uranyl acetate and lead citrate. All sections were cut using diamond knives and Ultracut S from Leica (Leica, Rueil-Malmaison, France). They were viewed with a JEOL Electron Microscope (JEOL, Tokyo, Japan) at 80 kV.

For immunoelectron microscopy, renal tissue was fixed and embedded according to Berryman and Rodewald [23]. Explanted metanephroi were fixed with the following solution: 4% paraformaldehyde (wt/vol), 0.1% glutaraldehyde (wt/vol), 0.2% picric acid (wt/vol), 0.15% tannic acid (wt/vol) and 0.5 mM calcium chloride in 0.1 M cacodylate buffer, pH 7.2. After extensive washes with ice-cold cacodylate buffer, specimens were stained *en bloc* with 2% uranyl acetate (wt/vol), and dehydrated in a series of graded aceton at −20°C and embedded in LR-Gold according to the manufacturer under light exposure with benzil as initiator. Ultrathin sections (~90 nm) were collected on Parlodion coated nickel grids and submitted to gentamicin immunodetection. Grids were rehydrated in Tris buffer saline (TBS), incubated first with 50 mM NH_4Cl in TBS, then with 0.5% serum (vol/vol) and 0.2% gelatin (wt/vol) in TBS, and exposed successively to mouse anti-gentamicin (BioDesign International, Kennebunkport, ME, USA) and colloidal-gold (10 nm) coupled goat anti-mouse (Biocell, Cardiff, UK) antibodies. All steps were performed by allowing the grids to float on drops of reagents. Control labeling experiments were carried out without either the first or the second antibody, using metanephroi exposed or not to gentamicin. Data are from four pairs of metanephroi for each time point.

Ureteric bud labeling

Filter grown metanephroi for 24 hours were fixed overnight with 2% paraformaldehyde in PBS, rinsed with PBS and incubated with 50 mM NH_4Cl for 30 minutes. Then, they were permeabilized with 0.075% saponin (wt/vol) that was kept throughout the labeling procedure, and stained with fluorescein-coupled *dolichos biflorus* agglutinin (DBA) with 0.2% gelatin (wt/vol) in PBS. After several washes, they were mounted in PBS/glycerol (vol/vol) containing 100 mg/ml of diacylbicyclooctane and 0.1% sodium azide, as previously described [17]. Observation was carried out on either an Optiphot epifluorescence microscope (Nikon, France) or a Biorad MRC-600 confocal microscope.

Confocal microscopy and image analysis

Six pairs of DBA-labeled explanted metanephroi were observed with a 10× objective (plan-Apo, numerical aperture = 0.45) and excited at 488 nm with an argon laser. For data collection, optical sections parallel to the filter were generated every 15 μm by the laser scanning confocal microsope Biorad MRC600. For each sample, 11 sections were performed. The files were then transferred to an Iris Indigo 4000 Entry workstation (Silicon Graphics, USA) and the image analysis was performed using Visilog 4.1.1. software (Noesis, France). The program was written under the C-Interpreter of Visilog. The main steps of the image analysis were the following:

(1) Segmentation of the "ureteric bud" and calculation of the skeletons. The 11 optical sections were cut with the same rectangular window which was defined as the analytical area. Each optical section was then analyzed as illustrated on Figure 1. Pixels were encoded on eight bits, so the dynamic of the image was represented by 256 grey levels (0 to 255) (Fig. 1A, raw data). Because of variations in the grey level range and the presence of discontinuous patches of labeled areas within the ureteric bud, it was almost impossible to select the ureteric bud with a simple thresholding (Fig. 1B). We therefore decided to realize the segmentation of the ureteric bud in three main steps: (i) after analysis of the pixel intensity histogram of the confocal image, the image background was manually monitored and the histogram was equalized between this value and the maximal value 255. This enhanced the image contrast (Fig. 1C); (ii) to reduce the local variations of staining intensity, the image was smoothed before thresholding (Fig. 1D, red line); (iii) the boundary of the binary image was smoothed (Fig. 1E) and the binary image was "skeletonized" (Fig. 1F). Superimposition of the skeleton on either the binary image (Fig. 1G) or on the original confocal image (Fig. 1H) demonstrates the accuracy of this technique.

(2) Calculation of the "mean skeleton" of the ureteric bud. The binary image of the skeleton of each optical section was converted and multiplied by 23, so that when the eleven skeletons were added to each other, the maximal grey level was 253 (11×23) (Fig. 2A). This image corresponds to the "mean skeleton" of the ureteric bud. In this image, the maximum grey level represents the maximum overlap between the eleven binary skeletons. To validate our approach, the "mean skeleton" was superimposed on the labeled ureteric bud (Fig. 2B), and the total length of the ureteric bud from the image of its skeleton was measured.

(3) Calculation of the number of "branching points" of the ureteric bud skeleton and analysis of their localization. The branching points of the mean skeleton image were calculated on the binary skeleton which was obtained after thresholding of the mean skeleton. The threshold value was > 46, corresponding to more than two overlaps of individual skeletons. Determination of the number of branching points was then performed, considering that a dichotomous division of the ureteric bud skeleton is a triple point, that is, a point with three neighboring points on the skeleton. All branching points were calculated, and the very close ones (< 6 pixels) were reduced to their centroid (Fig. 2C). To analyze their radial distribution between the first division of the ureteric bud and the external boundary of the explant represented on Figure 2D, a series of 20 concentric crowns was generated between these two lines (Fig. 2E). The growth of the ureteric bud and its branching pattern can consequently be analyzed in the whole metanephros organ culture, and the number of branching points assessed in each crown as depicted in Figure 2F.

(4) Contribution of successive ureteric bud branches on metanephros growth. Each branching point was perpendicularly projected on a growth axis defined by the orientation of the first branches of the ureteric bud, as depicted on Figure 11A (the same angle was measured in control and gentamicin groups). In this manner, for a given branching point of rank "i", the distance of the tubular segment that generated it ($d_{i-1,i}$) can be compared to the distance of the branch that emerged from this point to the next one ($d_{i,i+1}$). The ratio $d_{i-1,i}/d_{i,i+1}$ gives information on the contribution of the successive generations of branching points "i" to the growth of the ureteric bud, and the length of ($d_{i,i+1}$) being mostly dependent on its next branching ability. Data were analyzed in two areas, namely A and B, corresponding to the ureteric bud branches located above or below the axis, respectively.

Statistics

Data are reported as means with their standard errors. Comparisons between control and G50 groups were performed by the Wilcoxon's or Mann Whitney test. Significance was determined by $P < 0.05$.

Results

Growth and cell proliferation

At the time of explantation, E14 rat metanephroi had a ureteric bud that had divided about three times, with six to eight dilated tips interacting with the surrounding metanephric mesenchyme (Fig. 3A). Serial sectioning and histologic examination of these metanephroi indicated that the first recognizable nephron anlagen, namely the renal vesicles, were present in a central area, as previously observed [17]. In organ culture, metanephros grows flat and most of the dichotomous branching occurs in the plane of the permeable support. Throughout one day of culture, intense branching morphogenesis of the ureteric bud occurred and metanephrogenic cells around its ends continued to condense (Fig. 3B). Three to four days of culture are needed to visualize mature glomeruli.

Analysis of *in vitro* growth of E14 metanephroi was carried out after 1 and two days of culture in absence or in presence of 50 μg gentamicin/ml (G50). No difference in the protein content (μg/metanephros) was observed after 24 hours (8.1 ± 0.2 in controls vs. 7.8 ± 0.2 in G50, $N = 14$) and after 48 hours of culture (18.0 ± 0.7 in controls vs. 17.0 ± 0.5 in G50, $N = 14$). The surface area (mm^2) was also found to be the same in the control and experimental groups after 24 hours (0.67 ± 0.02 in controls vs. 0.67 ± 0.01 in G50, $N = 14$) and after 48 hours (1.39 ± 0.04 in controls vs. 1.33 ± 0.02 in G50, $N = 14$). Thus, the overall growth was the same in both culture conditions, and both parameters doubled every 24 hours. We then assessed the effect of gentamicin on cellular proliferation within explanted metanephroi (Fig. 4). The first eight hours of exposure to gentamicin had no effect on ^{3}H-thymidine incorporation in cultured metanephroi, but a significant reduction was detected at 24 hours of culture (-12.5%), and the effect was even more pronounced after 48 hours (-22.5%). However, no difference in DNA content per explant was detected as reported on the same figure. In the control and gentamicin groups, the cellular viability was greater than 95% after two days of culture.

Ultrastructural examination and gentamicin localization

As shown on Figure 5, gentamicin was detected in explanted metanephroi as soon as eight hours of drug exposure. In the ductal ureteric bud cells, gentamicin was mostly localized within large cytoplasmic vesicles and lysosomes, and was present on the apical surface (Fig. 5A). However, gentamicin was also detected in the end-bud cells, that is, within the cells that are engaged in morphogenetic interactions with the neighboring mesenchyme (Fig. 5 B, C). Despite this short exposure to gentamicin, numerous aggregates of induced mesenchymal cells engaged in epithelial conversion had already trapped gentamicin (Fig. 5 D, E). Regarding the uninduced metanephric blastema cells, few gold particles

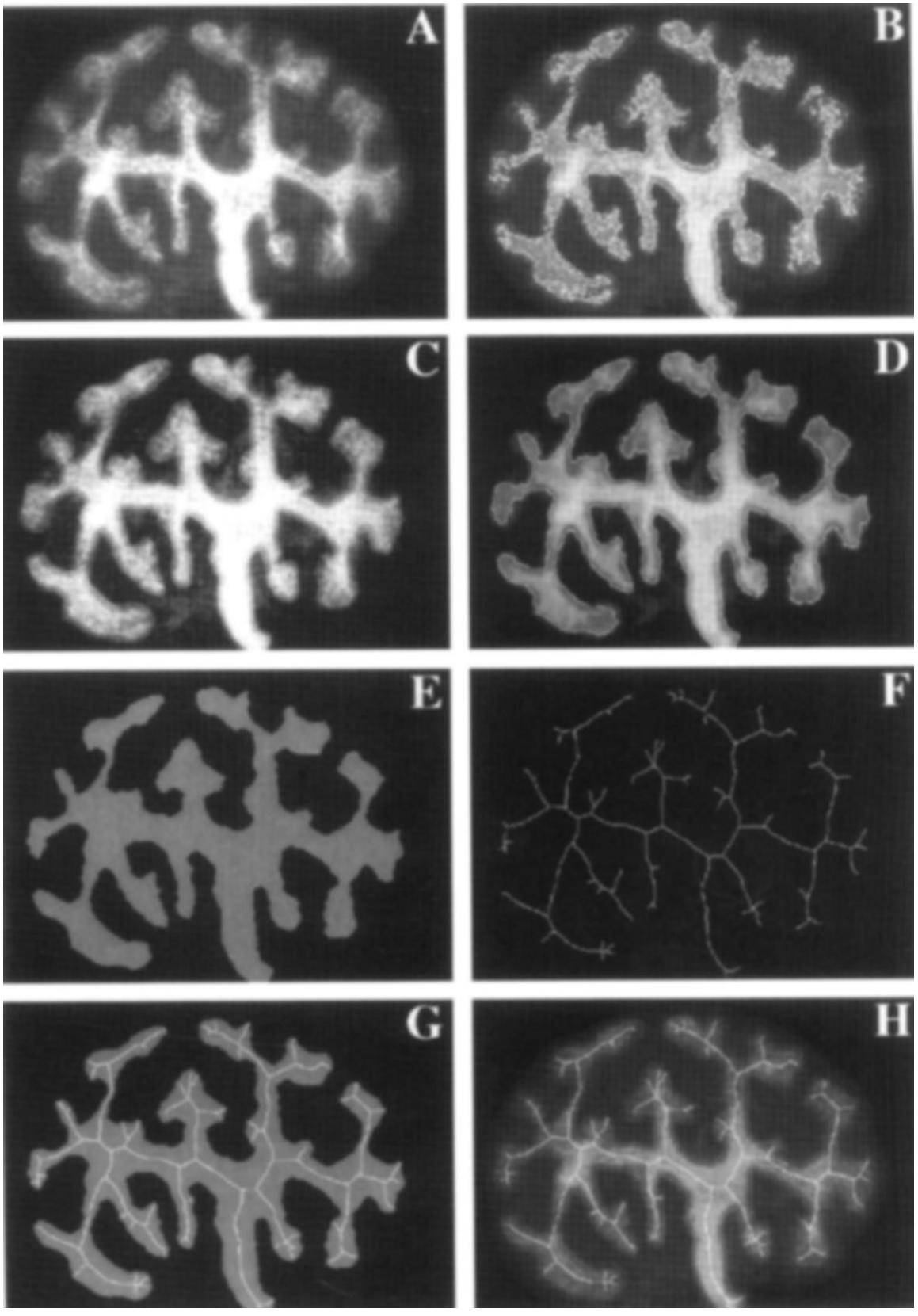

Fig. 1. *Analysis of the ureteric bud branching pattern from confocal images.* After specific labeling of the ureteric bud using FITC-coupled DBA, the skeleton of the ureteric bud was generated by segmentation (detailed in the text).

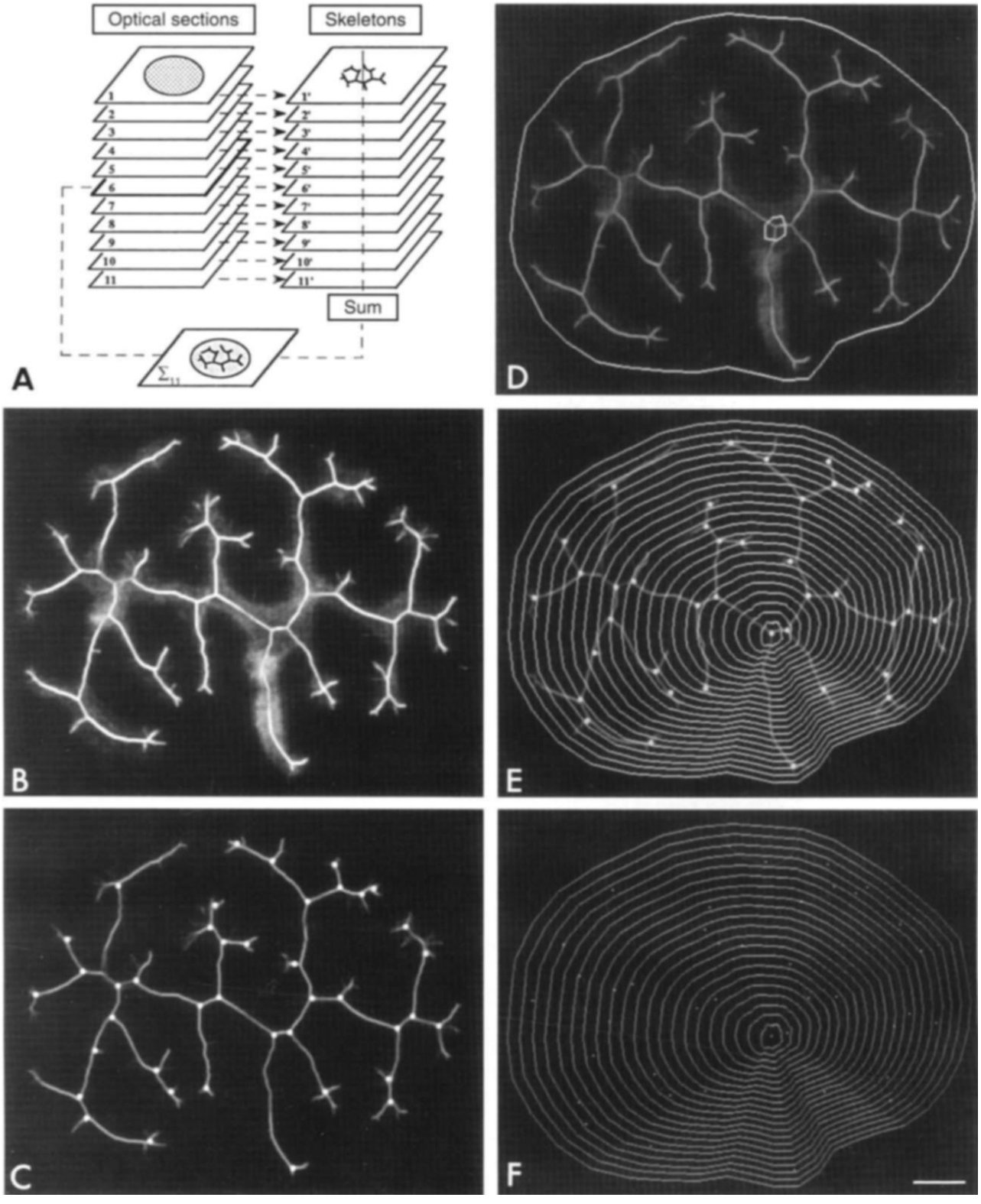

Fig. 2. *Determination of the number of branching points and analysis of their localization.* **A.** For each metanephros, generation of a series of 11 bud skeletons from the optical sections. **B.** Superposition of the median optical section to the mean skeleton. **C.** Calculation of the branching points from the mean skeleton. **D.** Identification of the first branching point area and of the external boundary of the explanted metanephros. **E.** Generation of 20 crowns between this two boundaries. **F.** Determination of the location of each branching point in every crown. Bar represents 150 μm.

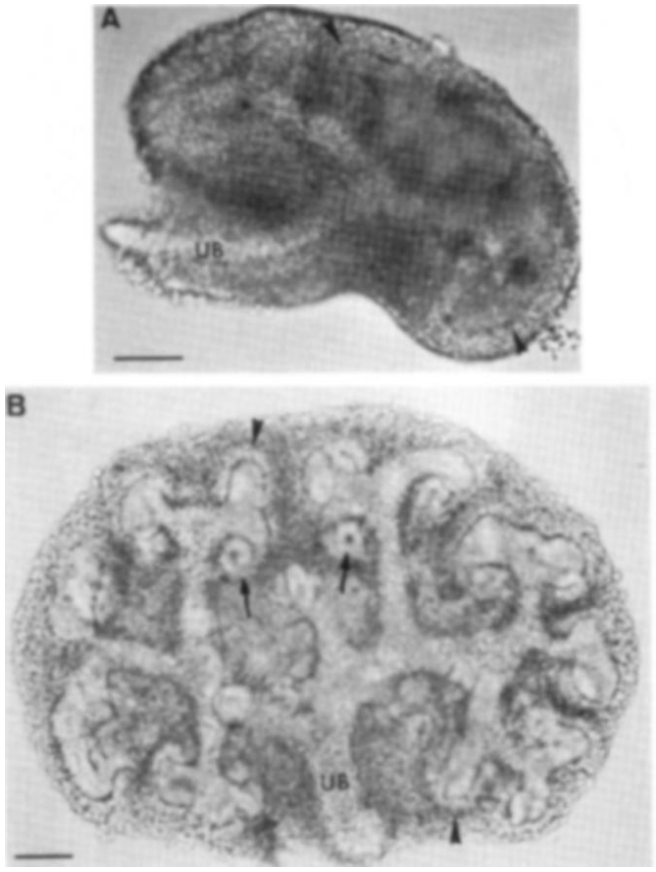

Fig. 3. *Photomicrographs of E14 rat metanephroi, freshly isolated (A) and after one day of culture in a serum-free chemically defined medium (B).* Explanted metanephroi were grown on a permeable filter and renal differentiation can pursue under these conditions. Arrowheads point to ureteric bud (UB) ends with a condense surrounding mesenchyme. Arrows indicate "S-shaped" bodies. Bar represents 100 μm.

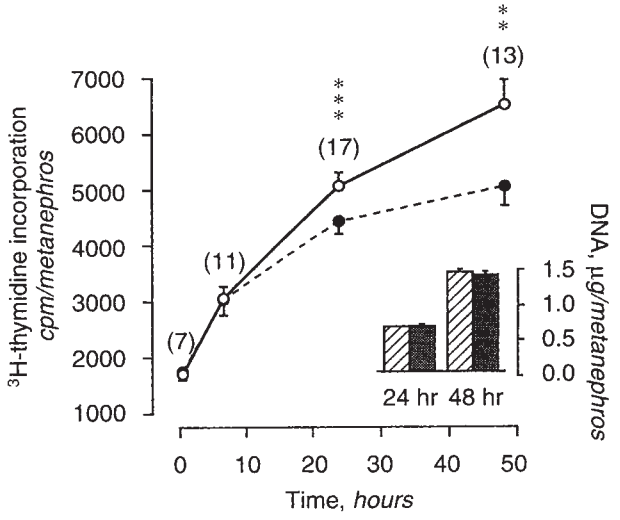

Fig. 4. *Thymidine incorporation and DNA content in E14 metanephroi grown without (○, ▨) or with gentamicin (●, ▩) for various period of time.* Numbers in parentheses represent the number of paired experiments performed at each time point. $^{**}P < 0.01$ and $^{***}P < 0.001$ as compared to controls.

were found intracellularly at this time, whereas the induced mesenchyme surrounding growing ureteric end buds contained numerous colloidal gold particles within cytosolic vacuoles. More developed renal anlagen such as renal vesicles also trapped the antibiotic (data not shown).

After 24 hours of contact with gentamicin, myelin-like membranous whorls (myeloid bodies) started to appear in various cellular compartments, both in the ureteric bud and in the metanephric blastema (Fig. 6 A, B). Gentamicin was localized with myeloid bodies that were frequently observed within large cytosegresomes in induced and uninduced cells. Ultrastructural analysis revealed that punctuate localization of gentamicin and myeloid bodies may also appear within mitochondria compartment and Golgi stacks (Fig. 6C). As expected, most of the lysosomes of the ductal bud cells contained gentamicin and myeloid bodies, as usually described for mature tubular epithelium cells exposed to aminoglycosides (data not shown). More surprising was the presence of cellular disorganization in the interactive zone between end buds and metanephrogenic mesenchyme (Fig. 6C).

By 48 hours of *in vitro* renal development after exposure to gentamicin, the extent of ultrastructural alterations in this interacting zone considerably increased (Fig. 7). Immunoreactive gentamicin was frequently detected over membrane-like debris and myeloid bodies within cytoplasmic vacuoles of the end bud cells (Fig. 7A). In controls, numerous foot-like processes and collagen fibrils established focal contacts between the ureteric bud and the renal mesenchyme (Fig. 7B), as reported *in vivo* [24]. Examination of the contralateral gentamicin-exposed metanephric explants showed a paucity of these intercellular connections and the presence of numerous vesicles with heterogenous material and myeloid bodies (Fig. 7C). In most of the mesenchymal cells, extension of the features depicted in Figure 6 was observed after the second day of gentamicin exposure, with increased density of gold particles.

Mitotic index in proliferative areas

Because gentamicin was shown (i) to be trapped within end buds and mesenchymal cells within eight hours of culture, (ii) to induce significant lesions between this two tissues, and (iii) to reduce the rate of thymidine incorporation from 24 hours onward, we explored whether or not the diminished rate of cell proliferation was related to a peculiar population of cells in the metanephros, that is, ureteric bud versus nephrogenic mesenchyme. We analyzed the percentages of cells engaged in mitosis in various areas of the ureteric bud and the surrounding blastema on metanephroi grown for 48 hours (Fig. 8). Gentamicin exposure had no effect on the rate of mitotic cells in the ductal ureteric bud and in the uninduced metanephric blastema. By contrast, the frequency of cells engaged in mitosis in the ureteric bud ends and in the induced mesenchyme was reduced by about 30% under gentamicin exposure.

Branching analysis of the ureteric bud

To visualize the ureteric bud, a specific labeling was obtained with fluorescein-coupled *dolichos biflorus* agglutinin in whole mount kidney rudiments that had been previously permeabilized (Fig. 9). The same staining intensity was observed for pairs of

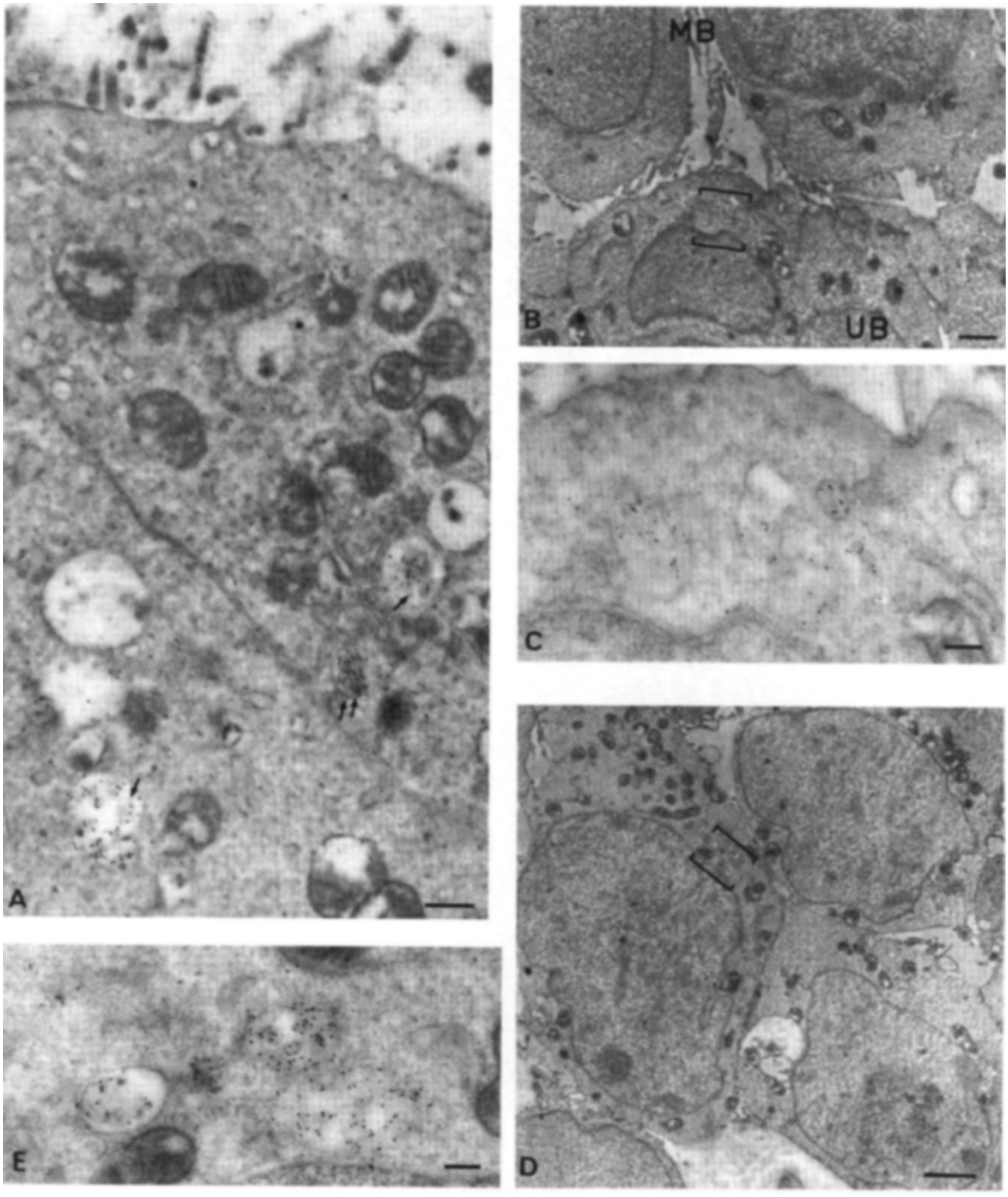

Fig. 5. *Immunogold localization of gentamicin on ultrathin sections of LR-gold embedded metanephros grown for eight hours with the antibiotic.* **A.** Epithelial cells of the ductal part of the ureteric bud exhibit numerous apical microvilli and endocytic vesicles. Gentamicin was detected within large cytosomes and lysosomes (arrows). **B.** Contact area between the metanephric blastema (MB) and one end of the ureteric bud (UB). The brackets indicate the location of the enlarged image, **C**, which reveals the presence of numerous gold particles within intracellular compartments of this distal ureteric bud cell. **D.** Cellular aggregates of induced metanephric cells with highly concentrated gentamicin in internal vesicles, as indicated in **E**, high magnification view of the area in brackets. No gold particle was found in control experiments. Bars represent 0.5 μm in A and C, 1 μm in B, 2 μm in D, and 0.2 μm in E.

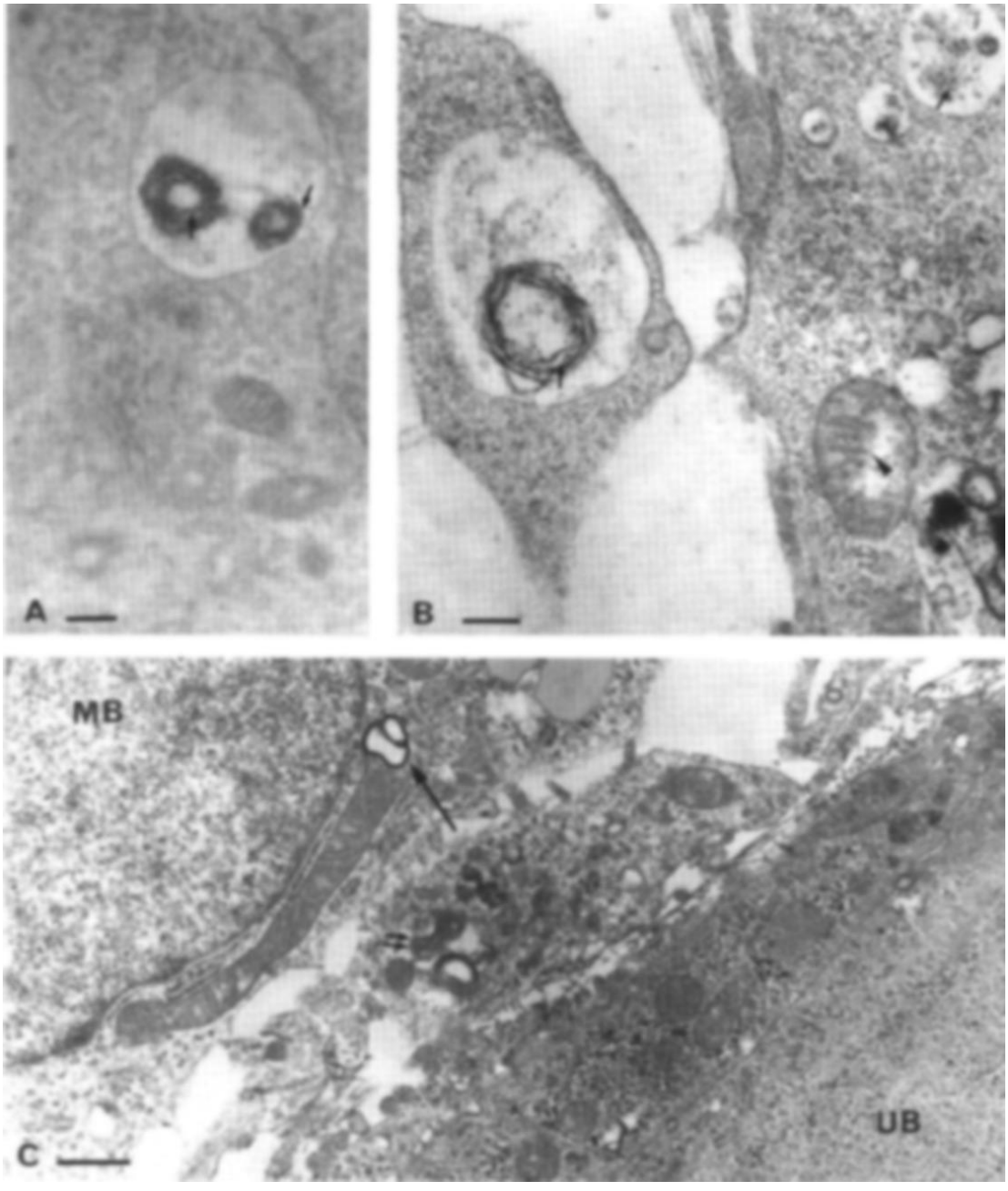

Fig. 6. *Electron micrographs of E14 metanephros exposed to gentamicin for 24 hours.* Immunogold gentamicin detection revealed abondant gold particles (arrows) in lysosomal compartment and over the myeloid bodies in both immature end bud cells (**A**) and uninduced metanephric mesenchyme (**B**). Some gold particles were also detected over mitochondria (arrowhead). **C**. Examination of the interacting zone between one end bud (UB) and the opposite mesenchyme (MB); myeloid bodies can be detected over mitochondrial (arrow) and Golgi stacks (double arrows) profiles. No gold particle was found in control experiments. Bars represent 0.5 μm in A and B, and 1 μm in C.

control and gentamicin-exposed metanephric explants grown for 24 hours. Differences in ureteric bud arborization seemed to have occurred depending on the presence or absence of gentamicin in the culture medium. To precisely assess the number and localization of branching points, as soon as they originated as "bumps" pushing out from the epithelial tubule, we analyzed the ureteric bud architecture using laser scanning confocal microscopy and image analysis as described in Figures 1 and 2. This was facilitated since metanephroi in organ culture are mostly two-dimensional in form. As illustrated on Figure 10A, the total length of the ureteric bud skeleton was not affected by the presence of gentamicin, and the same applied for surface measurement of the metanephros organ culture. However, the total number of branching points was significantly reduced upon 24 hours of gentamicin-exposure, as compared to controls. We then investigated if this defect was uniformely distributed in the kidney rudiment; the results are

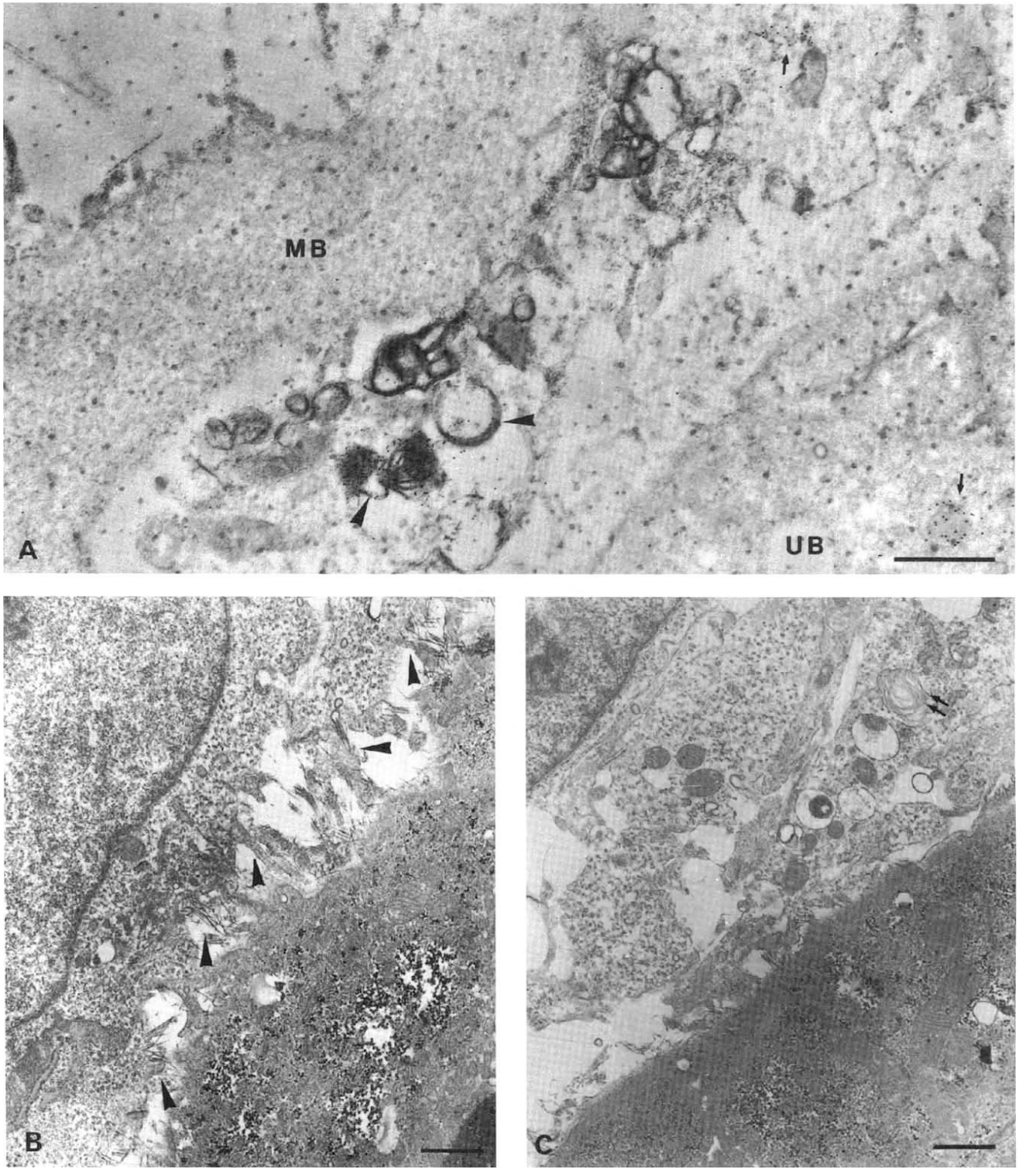

Fig. 7. *Examination of the interaction zone between the ureteric bud (UB) and the metanephric mesenchyme (MB) after two days of culture in absence* (**B**) *or presence of gentamicin* (**A, C**). **A.** Immunodetection of gentamicin on ultrathin LR-gold section: numerous gold particles are present over membranes whorls (arrowheads) and in large vacuoles or lysosomes, in both metanephric and terminal end bud cells (arrows). **B** and **C.** Ultrathin Epon sections showing a metanephrogenic cell (upper left) and end bud cell (lower right). A typical aspect of this area in control is given in B with many fibrillar and fuzzy materials, and cytoplasmic protrusions from both epithelial and mesenchymal cells (arrowheads). In C, cellular disorganization is present in this area, with almost no cytoplasmic processes from both tissue and many myeloid bodies (double arrows). Bars represent 1 μm in A, B, and C.

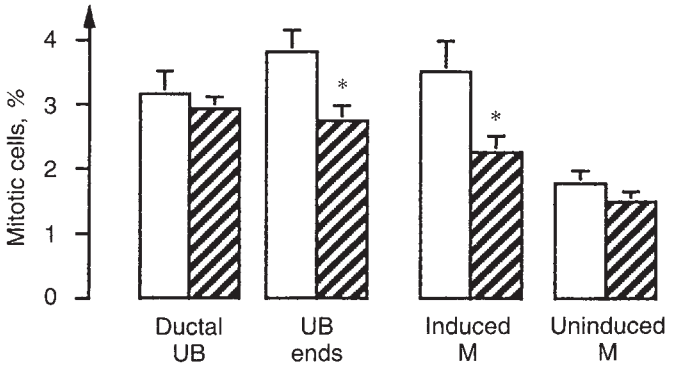

Fig. 8. *Determination of the mitotic cells in various area of the ureteric bud and the metanephric blastema after 48 hours of culture in absence (□) or presence of gentamicin (▨).* Four different areas have been studied: the ductal ureteric bud, ureteric end buds, the induced metanephric blastema, and the uninduced mesenchyme. Data are expressed as percentages of nuclear profiles engaged in mitosis. Abbreviations are: UB, ureteric bud; M, metanephric blastema. $^*P < 0.05$ as compared to controls.

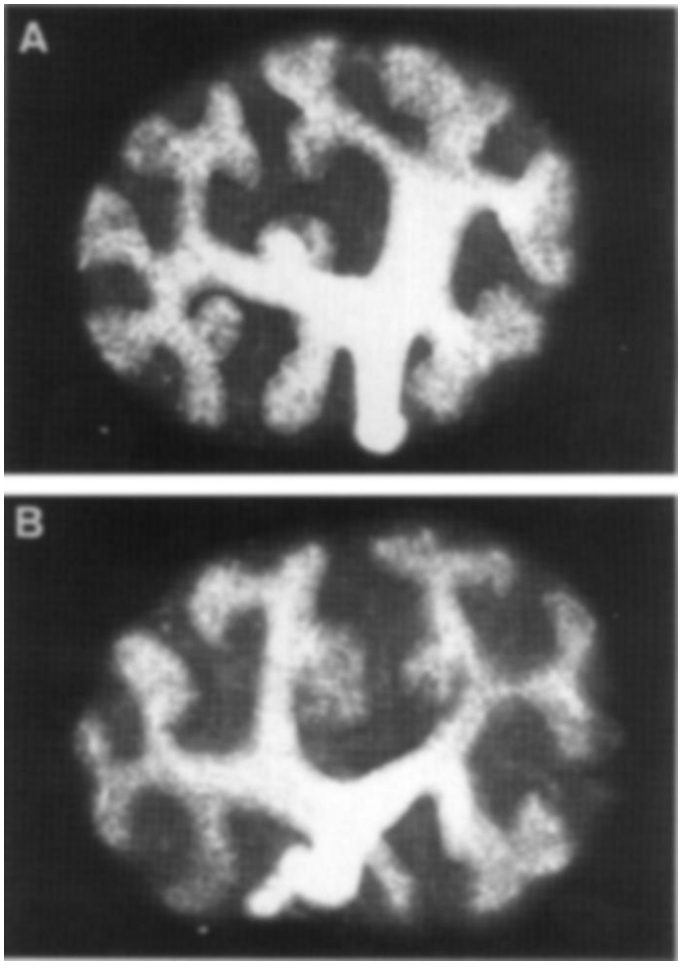

Fig. 9. *Visualization of the ureteric bud branches using FITC-coupled DBA in whole mount metanephroi grown for 24 hours in absence* (**A**) *or presence of gentamicin* (**B**). Both images are the projection of the eleven optical sections. Bar represents 100 μm.

shown on Figure 10B. First, it is worth noting that the 24 hours of *in vitro* metanephros development are represented by crowns #10 to #20, since at the time of explantation the size of the E14 metanephros fits more or less crown #10. Seven branching points can be counted up to this position, which is consistent with a ureteric bud that divided three times. Analysis of the number of branching points per crown in controls allowed us to show the successive waves of ureteric bud branching, and revealed that the fourth, fifth and sixth generations of bud division were localized in crowns #12, #15, and #18, respectively (Fig. 10B, inset). In gentamicin-exposed metanephros, a significant reduction in branching points appeared in crowns #12 and #15. However, because the number of branching points in crown #12 and #15 was not completely abolished, it suggested that some divisions of fourth and fifth generations did occur. In the four most external crowns, that is, #17 to #20, the number of branching events was of the same magnitude in both groups (11.3 ± 1.5 in controls vs. 10.2 ± 1.6 in G50, $N = 6$). The cumulative number of branching points was reduced in gentamicin-exposed metanephroi from rank #12 onwards.

Because the reduction in the number of branching points was not accompanied by a reduction of metanephros surface and of ureteric bud length, some end buds may have been elongated instead of engaged in branching process. In an attempt to verify this hypothesis and to specify which end buds might behave differently upon exposure to gentamicin, we analyzed the contribution of each end bud to metanephric explant growth, as schematized on Figure 11A. We showed that under control conditions, successive generations of branches contribute to various degrees to *in vitro* metanephros growth, the second and the fourth being the most effective, whatever the area of interest (Fig. 11B). In gentamicin-exposed metanephros, the growth profile of the ureteric bud in zone A parallels the controls. On the opposite, the presence of gentamicin clearly interfered with the ureteric bud growth in zone B. This is particularly evident for the fourth generation of branching event ("i" = 4). The ratio $d_{i-1,i}/d_{i,i+1}$ is significantly reduced by almost twofold. This suggests either the occurrence of a longer segment $d_{3,4}$ or a shorter $d_{4,5}$. Measurements of their length revealed that $d_{3,4}$ was longer, confirming that the fourth branching event was delayed in zone B in gentamicin-exposed metanephros.

Discussion

In the present study, we demonstrated that the disturbance of the ureteric bud branching morphogenesis may explain the mechanism through which gentamicin induces nephron deficit in metanephros organ culture. Remarkably, the ureteric bud branching pattern was altered within only 24 hours of culture, when none of the other growth parameters had yet been modified. The use of an elaborate ureteric bud analysis allowed us to show that the branching defect occurred between six (crown #12) and 12 hours (crown #15) of culture, which highlights the sensitivity of the ureteric end buds of fourth and fifth generation, respectively. By contrast, no branching defect occurred during the next 12 hours of culture (crowns #16 to 20), despite a period of intense arborization. The magnitude of the branching points defect was of about 18% when compared to the total number of divisions, but since it was generated between crowns 10 to 16, it represents a one third

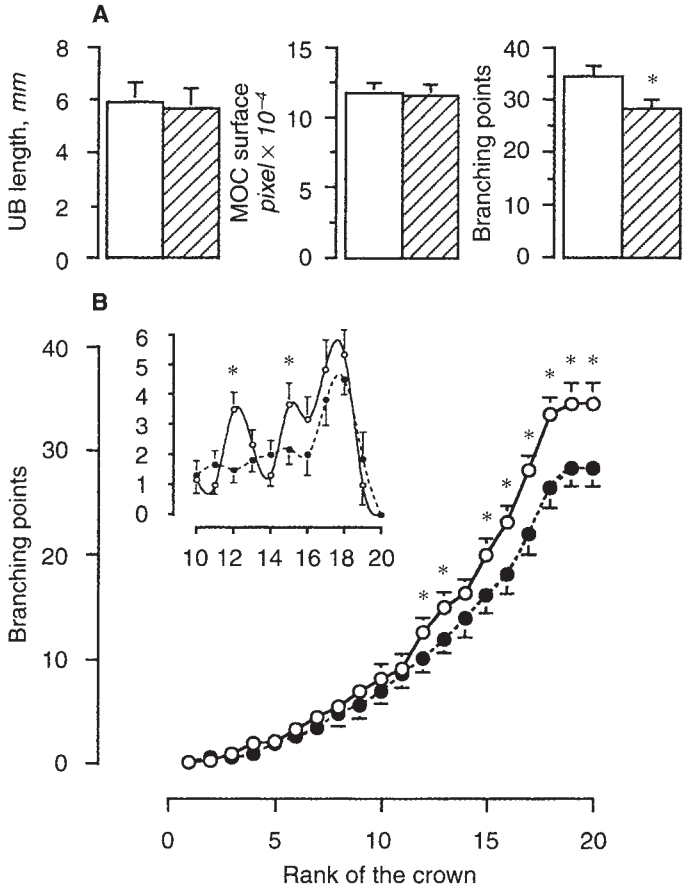

Fig. 10. *Morphometric analysis of E14 metanephroi grown in vitro for 24 hours.* **A.** Ureteric bud (UB) length, metanephros organ culture (MOC) surface, and the total number of branching points were determined in control (□) and in gentamicin-exposed kidney rudiments (▨). **B.** Distribution of the branching points of the ureteric bud in control (○) and gentamicin-exposed metanephroi (●). The small inset represents the number of branching points per crown for crown #10 to #20. In gentamicin-exposed metanephros, a significant reduction in branching points appeared in crowns #12 and #15. Below is represented the sum of branching events from the center of the explant (first crown) to the periphery (twentieth crown). From rank #12, a significant reduction of the total number of branching points appeared in the gentamicin group. Data are from six pairs of metanephroi. $^*P < 0.05$, as compared to paired controls.

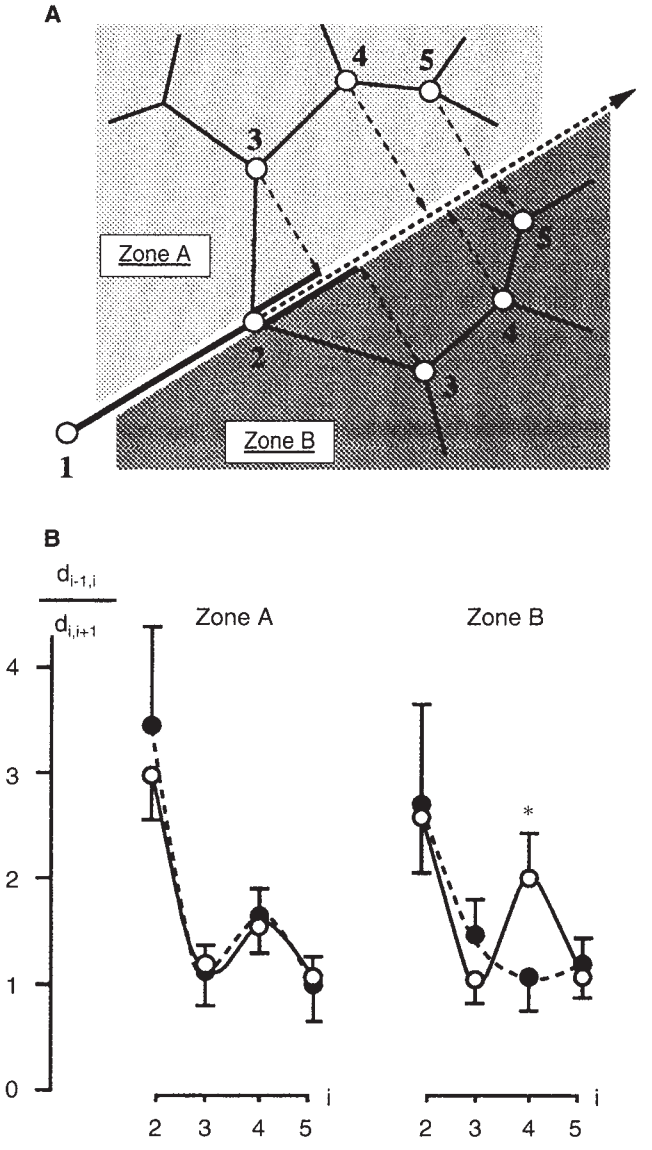

Fig. 11. *Contribution of the successive ureteric bud branches to the growth of the explanted metanephroi.* **A.** On this scheme, each branching point "i" was projected on the growth axis defined by the orientation taken by the first division of the ureteric bud. Numbers 1 to 5 represent the branching points of the first to fifth generations, respectively. Two zones of branching events were analyzed: zone A and zone B, above and below this axis, respectively. The distance between one branching point to the next one on this axis, namely $d_{i,i+1}$ or $d_{i-1,i}$, was measured. **B.** Measurement of the ratio $d_{i-1,i}/d_{i,i+1}$ for a branching point of generation "i" in each zone, in controls (○) and in gentamicin-exposed metanephros (●). This ratio gives information on the contribution of successive generations of branching point on the growth of explanted metanephros.

reduction of the branching events during this period. The reduction in branching morphogenesis is to the same extent as the reduction of nephrons we reported previously [16, 17].

Interestingly, ureteric bud end responsiveness to the aminoglycoside was heterogeneous depending on the area of bud development. During renal organogenesis, one of the first morphogenetic events is the division of the ureteric bud and the concomitant partition process of the mesenchyme mass around its newly formed ends [2]. This occurs several times before nephrogenesis begins. In E14 rat metanephros, nephron induction started in a central area opposite to the ureter (zone A), whereas lateral areas (zone B) remained free of renal anlagen. This was not a peculiar feature of rat kidney organogenesis. The same characteristics have been described in human kidney development where the first nephrons are induced by and attached to the third generation of end buds in the midpolar area (zone A), and to the fifth generation in the polar area (zone B) [1]. Thus, E14 rat metanephros containing a ureteric bud that branched only three times presented end buds in various configurations, some being committed to grow, some being engaged in dichotomous divisions, and others being involved in the nephron induction processes. The mesenchymal mass around each end may govern their various commitments and may also determine the position and direction

of the ureteric bud outgrowth. Thus, the budding-promoting activity controlled by the mesenchymal mass mentioned in many branching organs [5, 25–27] is likely to exist in the metanephros.

In this study, the elongation ability of the ureteric bud was not altered by gentamicin, at least by 24 hours, despite the uptake of large amounts of antibiotic by ureteric bud cells. This uptake confirms that collecting tubule anlagen possess the ability to incorporate the antibiotic. However, instead of the low uptake efficiency currently reported for adult collecting tubules [28, 29], we showed that the ureteric bud, a unique tubule with an epithelial phenotype in E14 rat metanephros, was the preferential site for gentamicin deposition. Regarding the branching commitment, the striking result is that it was impaired only in polar areas (zones B), where no nephrons have been formed yet, and that this defect was induced during the first twelve hours of culture. The presence of gentamicin there may have modified the mesenchymal mantle and then altered or delayed the transmission of signals controlling the balance between the epithelial and the mesenchymal components, leading to a modified branching signal. From a biophysical point of view, it is notable that gentamicin, unlike other aminoglycosides, has been shown to interact with the lipid bilayer by adopting an orientation parallel to the membrane and thus to create a diffusion barrier against ions or small molecules [30]. In the midpolar area, the absence of modifications of the ureteric bud branching suggests that the budding promoting activity of the mesenchymal mass is no more sensitive to the drug when nephrogenesis is turned on. This would also explain why the effect was transient, since after five divisions in the polar areas, end buds are involved in nephrogenesis. Regarding the nephron induction commitment, we believe that it was not affected by gentamicin since the number of nephrons we counted after four days of culture (which corresponded to the nephrons that have been induced within the first 24 hours of culture [17]) was reduced to the same extent as the branching points after 24 hours of gentamicin exposure. In an attempt to better resolve the changes in branching patterns due to gentamicin exposure, we tried to perform the same approach on kidney rudiments from E13 embryos. Unfortunately, pairs of such immature metanephroi, which have a ureteric bud that had branched once only, developed various branching patterns *in vitro* that prevented reliable comparisons.

The fact that growth and branching morphogenesis of the ureteric bud were differently affected by gentamicin reinforces the idea that these two processes may involve distinct signalling pathways and may thus be differently regulated, as has already been suggested [31]. Branching morphogenesis has been proposed to be controlled by protein serine/threonine phosphorylation via protein kinase C, while growth would be regulated by protein tyrosine phosphorylation via the scatter factor/c-met receptor [31]. Hagiwara et al reported that activity of protein kinase C is selectively inhibited by aminoglycosides [32]. Moreover, protein kinase C isoforms are known to be involved in the regulation of cell proliferation and differentiation [33]. Altogether this may provide some clues on how the branching defect is initiated. In addition to serine/threonine protein kinases, the phosphorylation state of target proteins can be regulated by serine/threonine protein phosphatases, the role of which has recently been demonstrated in early kidney development by Svennilson et al [34]. Their study also pointed towards the involvement of these phosphatases in regulating mitogenic activity, which might be consistent with the significant decrease of mitotic figures we observed in the morphogenetically active areas, since bud formation cannot proceed without proliferation [35]. The question of which pathway (branching vs. growth) predominates presumably depends on the presence and activation state of particular kinases, phosphatases and target proteins in end buds and mesenchymal cells.

The binding and uptake of gentamicin by eight hours of culture only within non-ductal ureteric end bud cells and the surrounding metanephric blastema are obviously the leading events of impaired branching morphogenesis. In mature epithelial cells, the toxicity of aminoglycosides depends on their accumulation within epithelial tubular cells, mostly in lysosomes, where they concentrate, induce phospholipidosis, and catalyze the formation of myeloid bodies [36–40]. The absence in end bud cells of a developed degradative compartment, the lysosome, may thereby expose other compartments, like those providing bioenergetic and synthetic pathways, to gentamicin toxicity, as previously proposed [15, 41]. For example, inhibitory effects of gentamicin on mitochondrial oxidative phosphorylation that have been reported to be an early pathogenetic event [42] may be significant in the initiation of the branching defect. However, whether or not an impaired signal from the mesenchyme and/or an altered response from the ureteric bud is the leading event of this defect remains to be solved. Upon prolonged gentamicin exposure, the occurrence of reduced epithelial-mesenchymal cell contacts and the appearance of membrane whorls between end buds and mesenchymal cells may explain the subsequent growth alteration [17], as suggested by the decrease of thymidine incorporation.

Data presented in this report demontrate that gentamicin-exposure results in the alteration of ureteric bud morphogenesis via branching modification without a change in elongation ability. Furthermore, the effect on branch initiation was limited to the polar area of the developing metanephros, where no nephron anlagen was present. Although the nature of molecular signals altered by gentamicin remains to be established, this study provides evidence that an aminoglycoside specifically interferes with the capacity of ureteric bud cells to push out as new bumps. The question arises whether similar findings might occur with other drugs that can cross the placenta and may interact with the differentiating metanephros. Finally, the morphometric analysis of the ureteric bud arborization we perfected represents the first quantitative approach of branching morphogenesis. The use of this approach should provide a better understanding of the role played by the ureteric bud in determining the renal architecture and in controlling the final number of nephrons, in normal and pathological renal organogenesis.

Acknowledgments

Preliminary reports of this work were presented at the Thirty Fifth Annual Meeting of the American Society for Cell Biology, New Orleans, USA, and at the First European Kidney Research Forum, Kloster Banz, Germany, and have been published in abstract form [43]. This work was supported by a grant from the Ministère de la Recherche et de l'Espace to T.G. (#92C-0457). The authors thank the University Paris 7-Denis Diderot and the Centre National de la Recherche Scientifique for the imagery department and the Centre Inter-universitaire de Microscopie Electronique for providing electron microscopy and photography facilities. We thank R. Schwarzmann from the Institut J. Monod for the confocal pictures.

Reprint requests to Thierry Gilbert, Ph.D, INSERM U.319, Université Paris 7, 2 place Jussieu, Tour 33-43, 75251 Paris Cedex 05, France. E-mail: TGilbert@Paris7.jussieu.fr

References

1. POTTER EL: *Normal and Abnormal Development of the Kidney*. Chicago, Year Book Medical Publishers, Inc., 1972
2. SAXÉN L: *Organogenesis of the Kidney*. Cambridge, Cambridge University Press, 1987
3. GROBSTEIN C: Inductive interaction in the development of the mouse metanephros. *J Exp Zool* 130:319–340, 1955
4. SPOONER BS, WESSELS NK: Mammalian lung development: Interactions in primordium formation and bronchial morphogenesis. *J Exp Zool* 175:445–454, 1970
5. WESSELS NK, COHEN JH: Early pancreas organogenesis: Morphogenesis, tissue interactions, and mass effects. *Dev Biol* 15:237–270, 1967
6. TAKAHASHI Y, NOGAWA H: Branching morphogenesis of mouse salivary epithelium in basement membrane like substratum separated from mesenchyme by the membrane filter. *Development* 111:327–335, 1991
7. CUNHA GR, ALARID ET, TURNER T, DONJACOUR AA, BOUTIN EL, FOSTER BA: Normal and abnormal development of the male urogenital tract–Role of androgens, mesenchymal-epithelial interactions, and growth factors. *J Androl* 13:465–475, 1992
8. GROBSTEIN C: Trans-filter induction of tubules in mouse metanephric mesenchyme. *Exp Cell Res* 10:424–440, 1956
9. EKBLOM P: Developmentally regulated conversion of mesenchyme to epithelium. *FASEB J* 3:2141–2150, 1989
10. BRENNER BM: Determinants of epithelial differentiations during early nephrogenesis. *J Am Soc Nephrol* 1:127–139, 1990
11. BRENNER BM: Nephron adaptation to renal injury or ablation. *Am J Physiol* 249:F324–F337, 1985
12. MERLET-BÉNICHOU C, LEROY B, GILBERT T, LELIÈVRE-PÉGORIER M: Intrauterine growth retardation and inborn nephron deficit. *Medecine/Sciences* 9:777–780, 1993
13. MERLET-BÉNICHOU C, GILBERT T, MUFFAT-JOLY M, LELIÈVRE-PÉGORIER M, LEROY B: Intrauterine growth retardation (IUGR) leads to a permanent nephron deficit in the rat. *Pediatr Nephrol* 8:175–180, 1994
14. HULTON SA, KAPLAN BS: Renal dysplasia associated with in utero exposure to gentamicin and corticosteroids–Brief clinical report. *Am J Med Genet* 58:91–93, 1995
15. GILBERT T, NABARRA B, MERLET-BÉNICHOU C: Light and electron microscopic analysis of the kidney in newborn rats exposed to gentamicin in utero. *Am J Pathol* 130:33–43, 1988
16. GILBERT T, LELIÈVRE-PÉGORIER M, MALIÉNOU R, MEULEMANS A, MERLET-BÉNICHOU C: Effects of prenatal and postnatal exposure to gentamicin on renal differentiation in the rat. *Toxicol* 43:301–313, 1987
17. GILBERT T, GAONACH S, MOREAU E, MERLET-BÉNICHOU C: Defect of nephrogenesis by gentamicin in rat metanephric organ culture. *Lab Invest* 70:656–666, 1994
18. BERNARD B, ABATE M, THIELEN PF, ATTAR H, BALLARD CA, WEHRLE PF: Maternal-fetal pharmacological activity of amikacin. *J Infect Dis* 135:925–932, 1977
19. BERNARD B, GARCIA-CAZARES SJ, BALLARD CA, THRUPP LD, MATHIES AW, WEHRLE PF: Tobramycin: Maternal-fetal pharmacology. *Antimicrob Agents Chemother* 11:688–694, 1977
20. AVNER ED, ELLIS D, TEMPLE T, JAFFE R: Metanephric development in serum free organ culture. *In Vitro* 18:675–682, 1982
21. AVNER ED, SWEENEY WEJ, PIESCO NP, ELLIS D: Growth factor requirements of organogenesis in serum-free metanephric organ culture. *In Vitro Cell Dev Biol* 21:297–304, 1985
22. LABARCA C, PAIGEN K: A simple rapid and sensitive DNA assay procedure. *Anal Biochem* 102:344–352, 1980
23. BERRYMAN MA, RODEWALD RD: An enhanced method for post-embedding immunocytochemical staining which preserves cell membranes. *J Histochem Cytochem* 38:159–170, 1990
24. LEHTONEN E: Epithelio-mesenchymal interface during mouse kidney tubule induction in vivo. *J Embryol Exp Morph* 34:695–705, 1975
25. ALESCIO T, COLOMBO PIPERNO E: A quantitative assessment of mesenchymal contribution to epithelial growth rate in mouse embryonic lung developing in vitro. *J Embryol Exp Morph* 17:213–227, 1967
26. MASTERS W JR: Epithelial-mesenchymal interaction during lung development: The effect of mesenchymal mass. *Dev Biol* 51:98–108, 1976
27. NOGAWA H, MIZUNO T: Mesenchymal control over elongating and branching morphogenesis in salivary gland development. *J Embryol Exp Morph* 66:209–221, 1981
28. MORIN JP, VIOTTE G, VANDEWALLE A, VAN HOOF F, TULKENS PM, FILLASTRE JP: Gentamicin-induced nephrotoxicity: A cell biology approach. *Kidney Int* 18:583–590, 1980
29. TOUBEAU G, MALDAGUE P, LAURENT G, VAAMONDE CA, TULKENS PM, HEUSON-STIENNON JA: Morphological alterations in distal and collecting tubules of the rat renal cortex after aminoglycoside administration at low doses. *Virchows Arch* 51:475–485, 1986
30. VAN BAMBEKE F, MINGEOT-LECLERCQ MP, SCHANCK A, BRASSEUR R, TULKENS PM: Alterations in membrane permeability induced by aminoglycoside antibiotics: Studies on liposomes and cultured cells. *Eur J Pharmacol* 247:155–168, 1993
31. DAVIES J, LYON M, GALLAGHER J, GARROD D: Sulphated proteoglycan is required for collecting duct growth and branching but not nephron formation during kidney development. *Development* 121: 1507–1517, 1995
32. HAGIWARA M, INAGAKI M, KANAMURA K, OHTA H, HIDAKA H: Inhibitory effects of aminoglycosides on renal protein phosphorylation by protein kinase C. *J Pharmacol Exp Ther* 244:355–360, 1988
33. CLEMENS MJ, TRAYNER I, MENAYA J: The role of protein kinase-C isoenzymes in the regulation of cell proliferation and differentiation. *J Cell Sci* 103:881–887, 1992
34. SVENNILSON J, DURBEEJ M, CELSI G, LAESTADIUS Å, DA CRUZ E, SILVA E, EKBLOM P, APERIA A: Evidence for a role of protein phosphatases 1 and 2A during early nephrogenesis. *Kidney Int* 48:103–110, 1995
35. GOLDIN G, HINDMAN H, WESSELLS N: The role of cell proliferation and cellular shape change in branching morphogenesis of the embryonic mouse lung: Analysis using aphidicorin and cytochalasins. *J Exp Zool* 232:287–296, 1984
36. SILVERBLATT FJ, KUEHN C: Autoradiography of gentamicin uptake by the rat proximal tubule cell. *Kidney Int* 15:335–345, 1979
37. KOSEK J, MAZZE R, COUSINS M: Nephrotoxicity of gentamicin. *Lab Invest* 30:48–57, 1974
38. PASTORIZA-MUNOZ E, BOWMAN RL, KALOYANIDES GJ: Renal tubular transport of gentamicin in the rat. *Kidney Int* 16:440–450, 1979
39. HUMES HD: Aminoglycoside nephrotoxicity. *Kidney Int* 33:900–911, 1988
40. LAURENT G, KISHORE BK, TULKENS PM: Aminoglycoside-induced renal phospholipidosis and nephrotoxicity. *Biochem Pharmacol* 40: 2383–2392, 1990
41. WILLIAMS PD, HOLOHAN PD, ROSS CR: Gentamicin nephrotoxicity. 1. Acute biochemical correlates in rats. *Toxicol Appl Pharmacol* 61:234–242, 1981
42. SIMMONS C, BOGURSKY R, HUMES H: Inhibitory effects of gentamicin of renal mitochondrial oxidative phosphorylation. *J Pharmacol Exp Ther* 214:709–715, 1980
43. GILBERT T, CIBERT C, MOREAU E, GAONACH S, GÉRAUD G, MERLET-BÉNICHOU C: Analysis of the branching pattern of the ureteric bud in cultured rat metanephroi with induced nephron deficit. *Mol Biol Cell* 4:146a, 1993